THE ASTROPHYSICAL JOURNAL, 493:762–774, 1998 February 1

A LOWER LIMIT TO THE DISTANCE OF HIGH-VELOCITY CLOUD COMPLEX H

BART WAKKER
Department of Astronomy, University of Wisconsin, 475 N. Charter Street, Madison, WI 53705; wakker@astro.wisc.edu
HUGO VAN WOERDEN
Kapteyn Astronomical Institute, Rijks Universiteit Groningen, Postbus 800, 9700 AV, Groningen, The Netherlands; hugo@astro.rug.nl
KLAAS S. DE BOER
Sternwarte, Universität Bonn, Auf dem Hügel 71, D-53121 Bonn, Germany; deboer@astro.uni-bonn.de
AND
PETER KALBERLA
Radioastronomisches Institut der Universität Bonn, Auf dem Hügel 71, D-53121 Bonn, Germany; kalberla@astro.uni-bonn.de
Received 1997 June 13; accepted 1997 September 9

ABSTRACT

We derive a lower limit for the distance of the high-velocity cloud (HVC) complex H, which is a structure covering 480 square degrees on the sky and is centered on $l = 131°$, $b = 1°$. Considering the uncertainties in the derivation of stellar distances, we find that the distance to the HVC is certainly larger than 3.4 kpc, probably larger than 5 kpc, and possibly larger than 6.5 kpc. This distance limit is based on the result that we do not find absorption associated with the HVC in *IUE* spectra of 17 OB stars. The three most distant of these stars were observed by us; we used the *IUE* archives to analyze the spectra of the other 14 stars. We do not have conclusive evidence that heavy elements are present in this HVC. This would require a detection of absorption in the spectrum of an extragalactic background source. However, the nondetections can still be considered secure, as the column density detection limits for the Mg II $\lambda\lambda$2796, 2802, C II λ1334, and O I λ1302 lines are a factor of 30–4100 below the column density values expected for normal interstellar medium gas phase abundances. Our lower limit to the distance is used to discuss possible origins of HVC complex H. It seems unlikely that it is associated with a superbubble at large Galactocentric radii, an infalling dwarf galaxy, or the outer arm. It might be an unusual Galactic fountain cloud or an intergalactic cloud.

Subject headings: Galaxy: halo — ISM: clouds — ISM: individual (HVC-H) — stars: distances — ultraviolet: ISM

1. INTRODUCTION

Since high-velocity clouds (HVCs) were discovered in 1963 (Muller, Oort, & Raymond 1963), they have been one of the more enigmatic components of the interstellar medium (see Wakker & van Woerden 1997 for a review). They can be defined as neutral hydrogen moving at velocities incompatible with a simple model of the distribution and rotation of galactic gas. HVCs are most easily recognized at high Galactic latitudes, where velocities relative to the LSR larger than 100 km s^{-1} always fall outside the range of velocities consistent with differential galactic rotation. On the other hand, for some longitudes in the Galactic plane such high velocities can be consistent with differential galactic rotation. Nevertheless, gas with incompatible velocities also exists in the plane. The most notable of the Galactic-plane HVCs is the one named complex H by Wakker & van Woerden (1991), which has velocities relative to the LSR between -120 and -210 km s^{-1}, more than 50 km s^{-1} more negative than can be understood from differential galactic rotation. It is centered at $l = 131°$, $b = 1°$, and was previously discussed by Hulsbosch (1971, 1975) under the name HVC 131+1−200. It is one of the largest HVCs, covering an area of 480 square degrees. Unlike some other large HVC complexes, it is not elongated but instead has a central concentration. A high-resolution map of this central condensation was included in the Westerbork study of Wakker & Schwarz (1991), who showed that the characteristics of the fine structure are similar to those observed in high-latitude HVCs. Wakker, Vijfschaft, & Schwarz (1991) used the Westerbork data to derive a spin temperature of 50 K for the core of this HVC. Since the line widths of the H I emission go down to 2.5 km s^{-1} for some of the simpler profiles, the kinetic temperature of the gas must be between 50 and 140 K. Knowledge of the distance to complex H is limited. Hulsbosch (1975) mentioned nondetections at the velocity of the HVC in Ca H and K spectra of 4 stars, with distances up to 3.6 kpc. He did not give the names of those stars, nor the implied abundance limits. Centurión et al. (1994) included eight stars projected onto complex H in their sample of Ca II and Na I observations. From the nondetections in their spectra, they claimed to derive a lower limit to the distance of 3.4 kpc. However, as explained in detail by Schwarz, Wakker, & van Woerden (1995), the interpretation of nondetections of absorption lines in stellar spectra is not always straightforward. A lower limit to the distance can only be found if the expected absorption strength is well above the noise level. A good estimate of the expected absorption strength requires a detection in the spectrum of an extragalactic object and an H I observation at the highest possible angular resolution toward both that extragalactic object and the star. The study of Centurión et al. (1994) suffered from these problems. The relevant 3 σ abundance limits for Ca^+ that they found were 1.7×10^{-9} toward Hiltner 198 (B1 V, distance 2.3 kpc) and 13×10^{-9} toward HD 10125 (O9.5 Ib, distance 3.4 kpc, their most distant star). Ca^+ has been detected toward five HVCs, with abundances ranging between 5×10^{-9} and 160×10^{-9}, with the median at 20×10^{-9}

(West et al. 1985; Robertson et al. 1991; Keenan et al. 1995; Schwarz et al. 1995; Wakker et al. 1996; see also Wakker & van Woerden 1997). Thus, of the detection limits derived by Centurión et al. (1994), only one was below the abundances observed elsewhere, so that only a distance limit of 2.3 kpc would have been reasonable. A major problem in the case of HVC complex H is that very few known extragalactic objects are projected on it, mostly because the high extinction near the galactic plane makes any such objects too faint. In the catalog of Véron-Cetty & Véron (1993), only seven extragalactic objects can be found projected onto complex H. The brightest of these is the QSO 4U 0241+61 ($B = 16$; Apparao et al. 1978). (The Véron-Cetty & Véron catalog gives $V = 12.2$, but that is an extinction-corrected estimate.) Other objects are fainter than $B = 17.5$. We have observed the Ca H and K spectrum of 4U 0241+61 and found a possible absorption due to complex H (U. J. Schwarz et al. 1997, in preparation). A definitive interpretation of a nondetection in a stellar spectrum in terms of a lower limit to the distance of a HVC will always require a determination of the abundance for the same ion from the spectrum of an extragalactic object. However, for UV resonance lines such as O I λ1302, C II λ1334, or Mg II $\lambda\lambda$2796, 2803, any absorption is usually deeply saturated, so one can be more confident that a nondetection corresponds to a lower distance limit, as we now show. The solar abundances of C and Mg are 3.5×10^{-4} and 3.8×10^{-5}, respectively (Anders & Grevesse 1989). In low-velocity gas, the logarithmic depletion ranges from about -0.15 to -0.4 for C and from -0.7 to -1.6 for Mg (Savage & Sembach 1996). Since under interstellar conditions the first ionization stage is usually dominant, for both C and Mg, this implies gas-phase abundances of 1.4–2.5×10^{-4} for $C^+$and of 1–8×10^{-6} for Mg^+. A 3 σ detection limit can be found from the formula given by Kaper et al. (1966) (see eq. [4] below), using a grid spacing of 5 km s^{-1}, an assumed intrinsic line width of 15 km s^{-1}, the fact that the resolution of the *IUE* spectra is $\sim$28 km s^{-1}, and assuming a signal-to-noise ratio (S/N) in the spectrum of 10. This gives 21 mÅ for C II and 48 mÅ for Mg II, which corresponds to 3 σ column density limits of about 10^{13} and 10^{12} cm^{-2}, respectively. In a direction where $N_{\rm H\,I}$ is at the limit of the HVC survey, i.e., 2×10^{18} cm^{-2}, the implied detection limits for the abundance are then 5×10^{-6} for C II and 5×10^{-7} for Mg II. Thus, even for a direction with low H I column density and maximal depletion, the expected absorptions are much stronger than the 3 σ detection limit in a spectrum with S/N of 10. Therefore, we selected the most distant known probes of complex H for observations with *IUE*. We further searched the *IUE* archives to expand the sample of probes and strengthen our conclusions. Section 2 describes the selection procedure, our observations, the archival search, as well as the estimation of stellar distances. Section 3 then describes the results and derivation of abundance limits. In Section 4 we derive a distance limit for complex H and discuss possible origins for the HVC that are consistent with this limit.

2. OBSERVATIONS

2.1. *Probe Selection*

As a first step, we created a list of possible probes, using many different star catalogs as input, choosing the "best" data for position, magnitude, colors, and spectral type. For complex H the most relevant catalogs are the Hipparcos Input Catalogue (Turon et al. 1992, usually giving the preferred spectral type) and the Smithsonian Astrophysical Observatory (SAO) Star Catalog (SAO Staff 1966, usually giving the coordinates). For the few stars that were not in the Hipparcos catalogue, the spectral types are found from the O-star catalog of Garmany, Conti, & Chiosi (1982), the list of Buscombe (1995), or the lists of Hardorp et al. (1959). Combining these catalogs, we obtained a spectral type, visual magnitude, and color for each star. We estimated the extinction by combining the spectral type (giving an intrinsic color) with the observed color. The intrinsic color for a given spectral type was found in Fitzgerald (1970), interpolating between types for cases not explicitly given. For stars earlier than O8, the colors of Walborn (1973) were used, as Fitzgerald does not give these. The visual extinction is then found as $3.2E(B-V)$. For a few stars for which $B-V$ was not given in the catalogs, the extinction map of Lucke (1978) was used to estimate the extinction. The distance was then estimated by combining the extinction estimate with the apparent magnitude and the absolute magnitudes for the given spectral type (from Straizys & Kurilene 1981). We discuss the accuracy of this estimate in § 2.3 below.

2.2. *Observations*

From the resulting list of probes we selected the best candidates for observing with *IUE* based on their distances and UV fluxes. Ultraviolet fluxes at $\lambda = 2800$ Å (near the Mg II doublet) and required exposure times were estimated from the visual magnitude, a differential ($\lambda - V$) extinction estimated to be equal to A_V, and the intrinsic magnitude difference $(\lambda - V)_0$, the latter being derived from the MK spectral type. Actual exposure times were further tailored to the net time available (about 6 hr per shift), given the amounts required for handover, maneuvering, target acquisition, and camera preparation. We obtained two *IUE* observing shifts of 8 hr, scheduled for 1993 November 16 and 17 at the ESA Satellite Tracking Station, Villafranca, Madrid, Spain. The LWP camera was used in high-dispersion mode and with the large aperture. Three stars could be successfully observed: HD 10125, BD +62 338, and BD +59 367. Since HVC complex H straddles the Galactic plane, it seemed likely that many OB stars projected onto it had previously been observed with *IUE*. We thus searched the *IUE* Merged Log for short-wavelength spectra (SWP camera) as well as long-wavelength spectra (LWP and LWR cameras) of all objects in a region with right ascension between 23^h20^m and 4^h40^m and declination between 40° and 80°. This box completely encloses HVC complex H. In Galactic coordinates its corners are at 105°, −19°; 119°, +18°; 162°, −4°; and 132°, +21°. The search was limited to spectra taken before 1995 December 31. The resulting list of 193 objects (1772 spectra) was correlated with the HVC catalog of Hulsbosch & Wakker (1988), and yielded a list of 361 SWP, 94 LWP, and 99 LWR spectra of 86 different objects projected onto complex H. We then compared the spectral types in our probe list with those given in SIMBAD. No major discrepancies were found. We did not find any stars significantly more distant than the three observed by us.

2.3. *Data Reduction*

From all stars observed with *IUE* projected onto complex H, we selected the O, B, and A stars for which the

distance estimate was larger than 1 kpc. This left 165 spectra (79 SWP, 39 LWP, 47 LWR) of 47 stars. All these spectra were fetched from the *IUE* archives and reduced using the package developed by the *IUE* Regional Data Analysis Facility (RDAF) at NASA/GSFC. Four spectra were not found by the software. The rest were converted from VAX to Unix format, which failed for five spectra. It is further useful to correct the velocities for the motion of the earth and the *IUE* satellite to get heliocentric velocities. For seven older spectra (taken before 1979) the header files did not contain sufficient information, and the velocity correction failed. (In general it is less than 20 km s^{-1}). We were thus left with 71 SWP, 36 LWP, and 42 LWR spectra of 45 stars. All 149 spectra (ours as well as archival) were plotted and inspected. We only kept those spectra that showed a straight continuum and sufficiently high S/N (>8). A few spectra in which a reseau mark happened to fall at the velocity of the HVC were removed. For four stars, more than one spectrum was taken with the same camera; these were averaged after inspection of the individual spectra. After all these steps, we were left with 24 spectra for 17 different stars. Figure 1 shows their positions on a map of the HVC complex. The parameters for these 17 stars are collected in Table 1. The numbers and integration times of the *IUE* spectra can be found in Table 2. The error in our derived stellar distances is difficult to estimate. For the final selection of probes the largest possible source of error is that the spectral type and luminosity class are wrong, which would imply a different intrinsic color and extinction. The observational values for magnitudes and colors are usually accurate to within 0.1 mag or better. If we assume that the spectral type can be at most one subtype and one luminosity class different from the actual value, we can calculate a range of possible distances for 13 of our 17 stars. The maximum uncertainty in the distance estimate is then about $\pm 25\%$. The possible range of the distance calculated this way is included in column (12) of Table 1.

2.4. H I *Spectra*

An estimate for the HVC velocities and brightness temperatures was obtained from the Dwingeloo survey for HVCs (Hulsbosch & Wakker 1988), by linear interpolation between the grid points of the survey. The resulting velocities and brightness temperatures are given in columns (15) and (16) of Table 1. To get the best determination of H I column density, one should in principle use a combination of Effelsberg (9′ beam) and Westerbork (1′ beam) observations (see Schwarz et al. 1995). However, only a few of the stars are in the field of a Westerbork observation. Effelsberg spectra exist toward most of the stars. These observations were calibrated against the IAU standard position S7 (Kalberla et al. 1982) and corrected for stray radiation (Kalberla et al. 1980). A third-order polynomial was fitted to the regions of the spectrum free from emission and interference and then subtracted. Next, we fitted a Gaussian to these spectra to derive the velocity, brightness temperature and line width of the HVC. The resulting values are given in columns (17)–(19) of Table 1. The spectra are presented in Figure 2. In that figure we also show the brightness temperature found from the interpolations applied to the Dwingeloo survey data, indicated by the "plus." This shows that there are significant differences between the profiles observed at 36′ and at 9′ resolution. However, usually these differences are less than a factor 2 in brightness temperature. The combination of brightness temperature (T_B) and line width (W) gives the H I column density in the

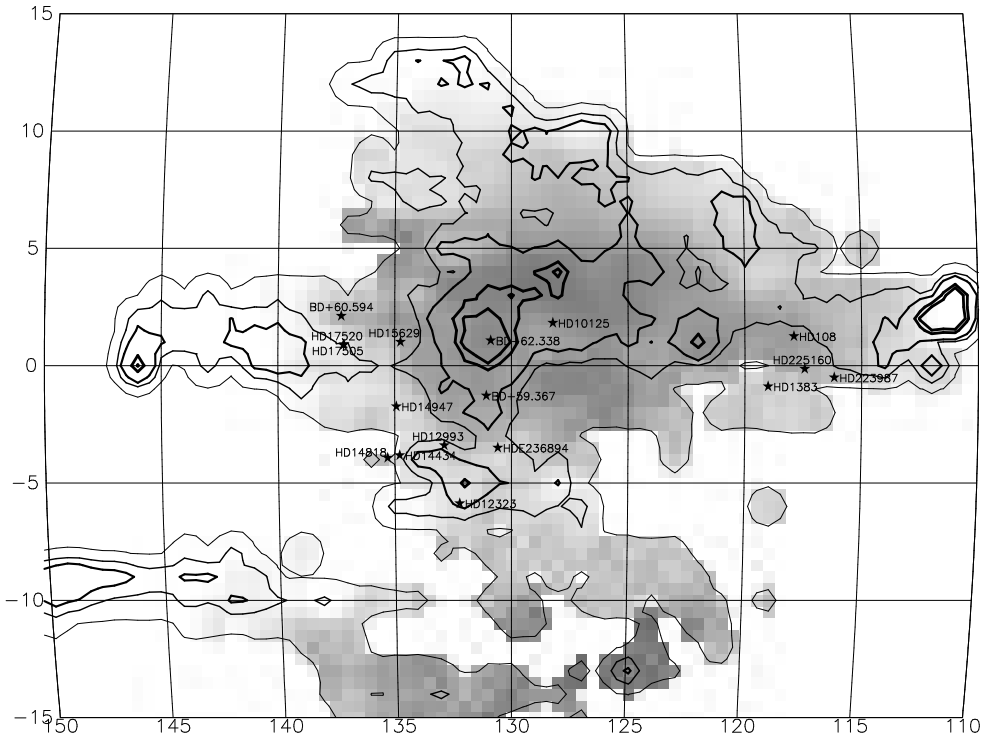

FIG. 1.—Positions of the final selection of stars, overlaid on a map of HVC complex H, using the H I data from the survey of Hulsbosch & Wakker (1988). Contour levels are at brightness temperatures of 0.05, 0.3, 0.6, 1, and 2 K. The corresponding H I column densities are about 3.6×10^{19} times the contour levels, assuming a line width of 20 km s^{-1}. The gray scale represents velocities, with the darkest areas at about -200 km s^{-1} and white areas at -100 km s^{-1}.

TABLE 1

STELLAR DATA

Star (1)	R.A. (2000) (2)	Decl. (3)	l (4)	b (5)	Type (6)	V (7)	$B-V$ (8)	$U-B$ (9)	A_V (10)	d (11)	d_{range} (12)	d_G (13)	v_r (14)	v_{HVC} (15)	T_{HVC} (16)	v_{HVC} (17)	T_{HVC} (18)	W (19)
BD +59 367.....	01 58 38.1	+60 30 55	131.11	−1.28	O9.5 I	9.77	0.53		2.6	5.0	3.6–7.5	6.5		−188	0.72	−183.2	0.30	26.1
BD +60 594.....	02 57 03.9	+61 24 58	137.38	2.12	O8.5 V	9.30	0.36	−0.64	2.1	2.6	2.1–3.4	2.2		−158	0.07			
														−188	0.09			
BD +62 338.....	02 02 11.4	+62 50 31	130.91	1.07	B3 II	9.22	0.21		1.2	3.6	1.2–6.0		−20	−199	3.86	−200.7	5.21	20.4
HD 108	00 06 03.3	+63 40 49	117.93	1.25	O6pe	7.38	0.18		1.6	1.7–2.6		2.5	−63	−190	0.19	−187.6	0.13	32.7
HD 1383	00 18 17.6	+61 43 38	119.02	−0.89	B1 II	7.63	0.27		1.6	1.7	0.9–2.6		−40	−160	0.23	−157.5	0.15	46.3
HD 10125.....	01 40 52.8	+64 10 25	128.29	1.82	O9.5 Ib	8.22	0.31		1.9	3.4	2.4–5.1	2.7	−38	−165	0.30	−162.0	0.32	21.5
														−204	0.54	−203.1	0.68	33.5
HD 12323.....	02 02 30.0	+55 37 27	132.91	−5.87	O9 V	8.91	−0.07		0.77	3.4	2.7–4.7	2.3		−146	0.49	−145.2	0.21	18.4
HD 12993.....	02 09 02.4	+57 55 56	133.11	−3.40	O6.5 V	8.97	0.22		1.7	3.4	3.1–4.1	2.3	−101	−141	0.17	−153.2	0.12	36.8
														−159	0.26			
HD 14434.....	02 21 52.3	+56 54 19	135.08	−3.82	O6.5 II	8.50	0.16	−0.79	1.5	3.8	3.2–4.6	2.3	−18	−165	0.03			
HD 14818.....	02 25 16.0	+56 36 37	135.62	−3.93	B2 Ia	6.25	0.30		1.5	2.4	1.3–2.4		−46	−168	0.05			
HD 14947.....	02 26 46.9	+58 52 34	134.99	−1.74	O5.5 If	7.98	0.46	−0.61	2.4	2.8	2.4–3.7	2.3	−56	−151	0.21	−149.4	0.30	31.8
HD 15629.....	02 33 20.4	+61 31 18	134.77	1.01	O5e	8.42	0.42		2.4	2.1–3.0		2.2	−40	−172	0.14			
HD 17505.....	02 51 08.1	+60 25 02	137.19	0.90	O6e	7.08	0.40		2.3	1.1–1.7		2.2	−20	−143	0.26	−141.1	0.18	32.9
HD 17520.....	02 51 14.5	+60 23 10	137.22	0.88	O8.5 II	8.26	0.32	−0.68	2.0	2.3	1.7–3.1	2.2	−34	−143	0.26	−140.5	0.18	52.3
HD 223987	23 54 13.1	+61 36 21	116.18	−0.51	B1 Ib	7.80			3.4	1.3	1.0–1.7			−170	0.13	−161.1	0.26	23.5
HD 225160	00 04 03.6	+62 13 20	117.44	−0.14	O8e	8.20	0.26		1.8	1.8–3.1		4.1	−45	−176	0.16	−172.4	0.14	35.2
HDE 236894.....	01 52 13.7	+58 26 07	130.83	−3.50	O8 V	9.38	0.19		1.6	3.4	2.9–4.5	2.3	−38	−162	0.40	−184.1	0.23	24.1

NOTE—Col. (1): Name of star. Cols. (2), (3): Right ascension and declination for equinox 2000. Cols. (4), (5): Galactic longitude and latitude. Col. (6): Spectral type. Col. (7): V magnitude. Cols. (8), (9): $B-V$ and $U-B$. Col. (10): Extinction A_v, estimated as $3.2E(B-V)$, where $E(B-V)$ is found from the given $B-V$ color and the intrinsic color for the given spectral type. Col. (11): Best estimate for the distance, as described in § 2.1; if two values are given, the second is an alternative estimate for the distance, for stars for which no luminosity class is known—then the first value gives the distance estimate assuming luminosity class V, the second assuming class II. Col. (12): Possible range in distance if spectral type is wrong by one subtype and one luminosity class. Col. (13): Distance given for the star in the catalog of Garmany et al. 1982, which takes into account membership of open clusters. Col. (14): Radial velocity of the star. Cols. (15), (16): LSR velocity and brightness temperature of the HVC at the position of the star, interpolated between the grid points of the Hulsbosch & Wakker 1988 survey. Cols. (17)–(19): LSR velocity, the brightness temperature, and FWHM of the HVC at the position of the star, as determined by a Gaussian fit to the profile observed at Effelsberg.

TABLE 2

IUE SPECTRA

Star	Spectrum	Date (Year Day)	t_{int} (min)
BD +59 367.....	LWP26770	1993 321	372
BD +60 594.....	LWR14834	1982 348	180
BD +62 338.....	LWP26763	1993 320	237
HD 108	LWR10537	1981 126	20
HD 108	SWP13910	1981 126	25
HD 108	SWP02126	1978 208	28
HD 108	SWP02386	1978 236	40
HD 108	SWP08352	1980 084	55
HD 1383	LWR07276	1980 083	30
HD 10125.....	LWP26762	1993 320	100
HD 12323.....	LWR12495	1982 033	27
HD 12993.....	SWP15277	1981 289	105
HD 12993.....	SWP16108	1982 025	200
HD 12993.....	SWP16238	1982 032	141
HD 14434.....	SWP16094	1982 022	90
HD 14818.....	LWR08161	1980 184	17
HD 14947.....	SWP10724	1980 336	360
HD 15629.....	SWP10754	1980 339	300
HD 17505.....	LWR14835	1982 348	70
HD 17520.....	LWP23636	1992 218	60
HD 17520.....	LWP24700	1993 010	60
HD 223987	LWR10076	1981 065	80
HD 225160	LWR09318	1980 321	70
HDE 236894.....	SWP53127	1994 353	335

direction of the probe. For the two probes for which no Effelsberg spectrum is available the Dwingeloo survey data are used, assuming a line width of 25 km s^{-1}. Assuming a Gaussian profile and low optical depth, the column density is given by

$$N_{\rm HI} = 1.823 \times 10^{18} \sqrt{\frac{\pi}{4 \ln 2}}\, T_B W \,. \quad (1)$$

3. RESULTS

3.1. *Expected Line Strengths*

In order to judge the significance of a nondetection of one of the UV lines, it is necessary to estimate the expected line strength. We can estimate the column density of the ion from

$$N(\text{ion}) = \delta A_{\odot} N_{\rm HI} \,. \quad (2)$$

Here $A_{\odot}$ is the solar abundance $[(X/H)_{\odot}]$, taken from Anders & Grevesse (1989). δ combines the effects of ionization and depletion onto dust grains (Jenkins 1987). To determine δ for the relevant ions (C^+, O^0, and Mg^+, see below), we use the abundance determinations for low-velocity gas recently obtained from high-quality *Hubble Space Telescope* data for several representative sightlines;

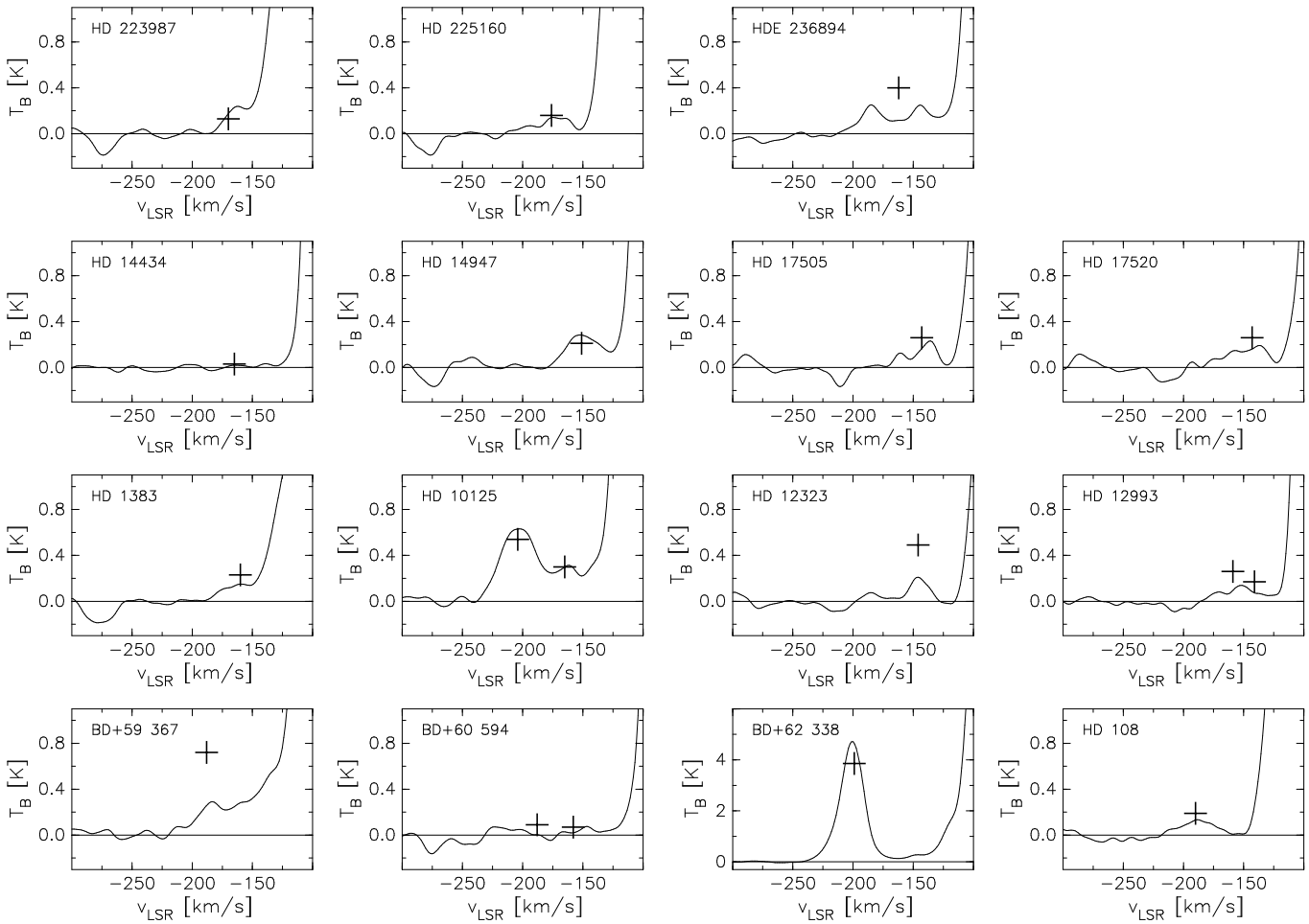

FIG. 2.—Effelsberg spectra (9′ beam) for 15 of the stars. The vertical scale has been enlarged to show the HVC, so that the low-velocity gas is off-scale. The cross indicates the velocity and brightness temperature found in the Dwingeloo HVC survey.

TABLE 3

LINE DATA

Element	$A_{\odot}$[a]	δ[b]	λ	f	rms Range[c]
C II.....	3.5×10^{-4}	0.39	1334.5323	0.1278	1310–1325
O I.....	7.4×10^{-4}	0.35	1302.1685	0.0504	1310–1325
Mg I	3.8×10^{-5}	0.0093	2852.9642	1.730	2854–2880
Mg II.....	3.8×10^{-5}	0.093	2796.3520	0.629	2815–2830
			2802.5310	0.314	2815–2830

[a] Solar abundance $[(X/H)_{\odot}]$ from Anders & Grevesse 1989.

[b] Product of depletion and ionization; C II: Cardelli et al. 1996; O I: Meyer et al. 1994; Mg II, assumed $N(\mathrm{Mg\ I})/N(\mathrm{Mg\ II}) = 0.1$: Fitzpatrick 1997.

[c] Wavelength range over which rms was calculated to determine detection limits.

they are given in Table 3, which also includes the values for the solar abundance of each element. It is possible that for HVCs δ is larger or smaller by a large amount, although at present there are insufficient data to determine this. Combining the $A_{\odot}$ and δ with the H I column density, we obtain a prediction for the column density of the ion. This column density can be converted into a peak optical depth. If we use an FWHM (Γ) for the absorption of 15 km s^{-1}, as suggested by the Ca II absorption profiles measured in several HVCs (Robertson et al. 1991; Keenan et al. 1995; Schwarz

TABLE 4

DETECTION LIMITS[a]

Star (1)	v_{LSR} (km s^{-1}) (2)	$N_{\mathrm{H\,I}}$ (cm^{-2}) (3)	Ion (4)	S/N (5)	N_{pred} (cm^{-2}) (6)	3 $\sigma(W)$ (mÅ) (7)	3 $\sigma(N)$ (cm^{-2}) (8)	3 $\sigma(A)$ (9)	3 $\sigma(\delta)$ (10)	S (11)
BD +59 367.....	−188	1.5×10^{19}	Mg II 2796	14	5.4×10^{13}	36	8.3×10^{11}	5.5×10^{-8}	0.0014	200
			Mg I 2852	10	5.4×10^{12}	49	4.0×10^{11}	2.6×10^{-8}	0.00069	40
BD +60 594.....	−158	3.4×10^{18}	Mg II 2796	21	1.2×10^{13}	23	5.4×10^{11}	1.6×10^{-7}	0.0041	67
			Mg I 2852	17	1.2×10^{12}	30	2.4×10^{11}	7.1×10^{-8}	0.0019	15
	−188	4.4×10^{18}	Mg II 2796	21	1.5×10^{13}	23	5.4×10^{11}	1.2×10^{-7}	0.0032	87
			Mg I 2852	17	1.5×10^{12}	30	2.4×10^{11}	5.5×10^{-8}	0.0015	19
BD +62 338.....	−199	2.1×10^{20}	Mg II 2796	22	7.3×10^{14}	23	5.3×10^{11}	2.6×10^{-9}	0.000068	4100
			Mg I 2852	18	7.3×10^{13}	28	2.2×10^{11}	1.1×10^{-9}	0.000029	980
HD 108	−190	8.2×10^{18}	Mg II 2796	22	2.9×10^{13}	22	5.2×10^{11}	6.3×10^{-8}	0.0016	170
			Mg I 2852	20	2.9×10^{12}	25	2.0×10^{11}	2.5×10^{-8}	0.00065	43
			C II 1334	8	1.1×10^{15}	32	1.6×10^{13}	1.9×10^{-6}	0.0055	210
			O I 1302	8	2.2×10^{15}	31	4.2×10^{13}	5.0×10^{-6}	0.0068	160
HD 1383	−160	1.3×10^{19}	Mg II 2796	21	4.8×10^{13}	23	5.4×10^{11}	4.0×10^{-8}	0.0011	270
			Mg I 2852	19	4.8×10^{12}	26	2.1×10^{11}	1.6×10^{-8}	0.00042	67
HD 10125.....	−165	1.3×10^{19}	Mg II 2796	28	4.7×10^{13}	18	4.1×10^{11}	3.1×10^{-8}	0.00081	350
			Mg I 2852	26	4.7×10^{12}	19	1.5×10^{11}	1.2×10^{-8}	0.00031	92
	−204	4.4×10^{19}	Mg II 2796	28	1.6×10^{14}	18	4.1×10^{11}	1.0×10^{-8}	0.00024	1100
			Mg I 2852	26	1.6×10^{13}	19	1.5×10^{11}	3.5×10^{-9}	0.000092	300
HD 12323.....	−146	7.5×10^{18}	Mg II 2796	22	2.7×10^{13}	22	5.1×10^{11}	6.9×10^{-8}	0.0018	160
			Mg I 2852	16	2.7×10^{12}	32	2.6×10^{11}	3.5×10^{-8}	0.00092	31
HD 12993.....	−141	1.0×10^{19}	C II 1334	8	1.2×10^{15}	31	1.6×10^{13}	1.8×10^{-6}	0.0052	230
			O I 1302	8	2.3×10^{15}	30	4.1×10^{13}	4.8×10^{-6}	0.0064	170
	−159	1.0×10^{19}	C II 1334	8	1.2×10^{15}	31	1.6×10^{13}	1.8×10^{-6}	0.0052	230
			O I 1302	8	2.3×10^{15}	30	4.1×10^{13}	4.8×10^{-6}	0.0064	170
HD 14434.....	−165	1.5×10^{18}	C II 1334	9	2.0×10^{14}	27	1.4×10^{13}	1.0×10^{-5}	0.027	44
			O I 1302	9	3.8×10^{14}	27	3.6×10^{13}	2.5×10^{-5}	0.033	32
HD 14818.....	−168	2.4×10^{18}	Mg II 2796	24	1.0×10^{13}	21	4.9×10^{11}	2.0×10^{-7}	0.0053	53
			Mg I 2852	26	1.0×10^{12}	20	1.6×10^{11}	6.5×10^{-8}	0.0017	16
HD 14947.....	−151	1.9×10^{19}	C II 1334	5	2.6×10^{15}	44	2.2×10^{13}	1.2×10^{-6}	0.0034	340
			O I 1302	5	4.9×10^{15}	43	5.8×10^{13}	3.1×10^{-6}	0.0042	250
HD 15629.....	−172	6.8×10^{18}	C II 1334	6	1.0×10^{15}	42	2.2×10^{13}	3.2×10^{-6}	0.0090	130
			O I 1302	6	1.8×10^{15}	41	5.6×10^{13}	8.3×10^{-6}	0.011	95
HD 17505.....	−143	1.1×10^{19}	Mg II 2796	23	4.1×10^{13}	22	5.1×10^{11}	4.4×10^{-8}	0.0012	240
			Mg I 2852	27	4.1×10^{12}	19	1.5×10^{11}	1.3×10^{-8}	0.00035	79
HD 17520.....	−143	1.0×10^{19}	Mg II 2796	36	3.6×10^{13}	14	3.1×10^{11}	3.1×10^{-8}	0.00082	340
			Mg I 2852	31	3.6×10^{12}	16	1.3×10^{11}	1.3×10^{-8}	0.00034	82
HD 223987	−170	1.2×10^{19}	Mg II 2796	30	4.2×10^{13}	16	3.8×10^{11}	3.2×10^{-8}	0.00084	330
			Mg I 2852	23	4.2×10^{12}	22	1.8×10^{11}	1.5×10^{-8}	0.00040	70
HD 225160	−176	1.0×10^{19}	Mg II 2796	27	3.4×10^{13}	19	4.3×10^{11}	4.5×10^{-8}	0.0012	240
			Mg I 2852	20	3.4×10^{12}	25	2.1×10^{11}	2.1×10^{-8}	0.00057	50
HDE 236894.....	−162	1.1×10^{19}	C II 1334	8	1.5×10^{15}	30	1.5×10^{13}	1.4×10^{-6}	0.0040	290
			O I 1302	8	2.8×10^{15}	29	3.9×10^{13}	3.6×10^{-6}	0.0049	220

[a] See § 3.2 for an explanation of the columns.

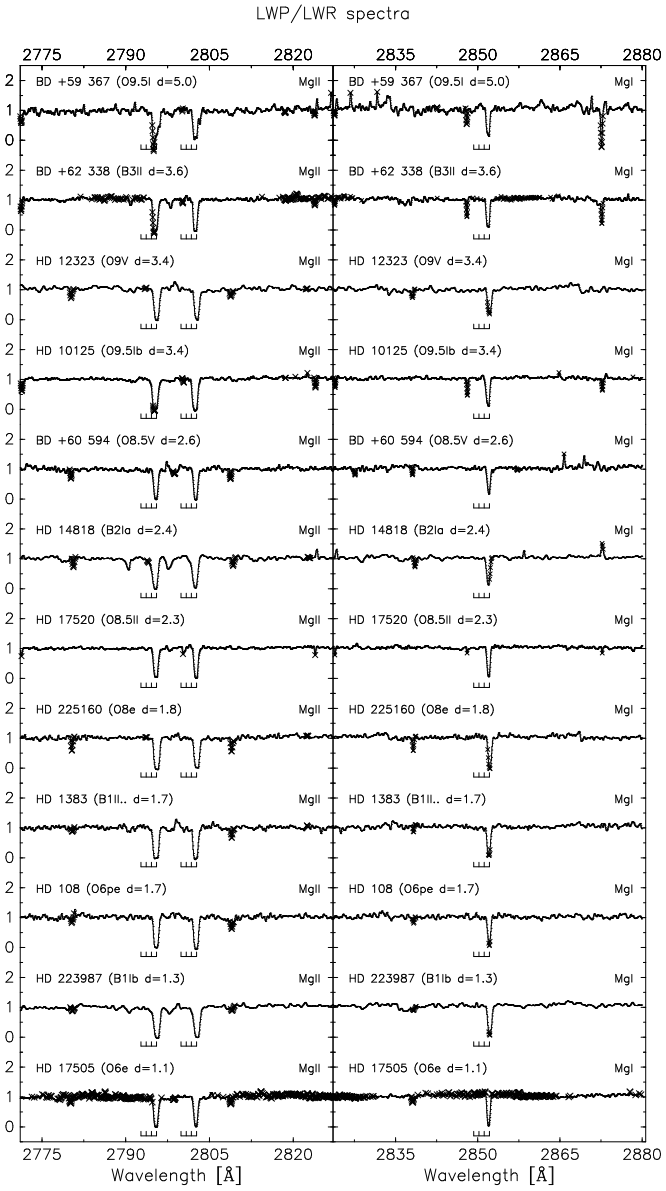

FIG. 3*a*

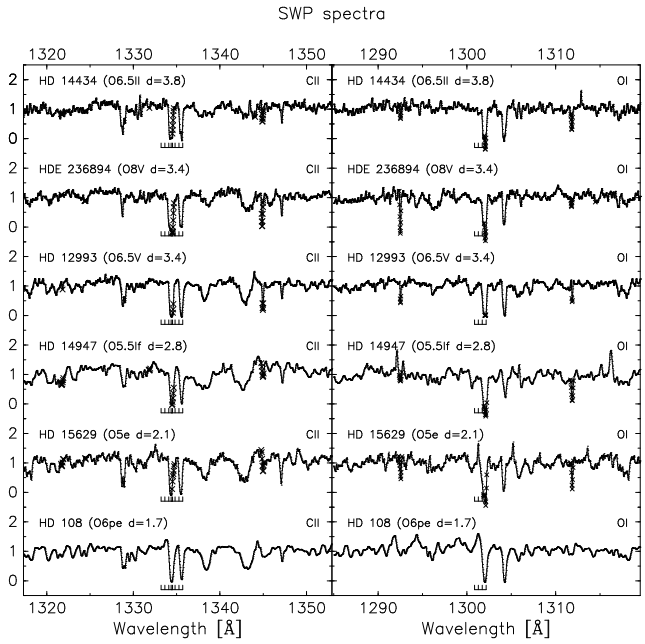

FIG. 3*b*

FIG. 3.—Regions around the selected spectral lines for each of the stars in the final sample. These show that confusing stellar lines are not present in the areas around the interstellar lines of interest. The four tick marks below each of the selected lines indicate LSR velocities of 0, −100, −200, and −300 km s^{-1} relative to the rest wavelengths. LWP or LWR spectra are shown in Fig. 3*a* and SWP spectra in Fig. 3*b*. The stars are sorted in order of descending distance, with the most distant star on top. Data points that are crossed out were marked as unreliable by the RDAF reduction software, most often because of the presence of a reseau mark.

et al. 1995; Wakker et al. 1996), the optical depth at the center of an absorption line is given by

$$\tau_0 = \frac{\pi e^2}{m_e c} f\lambda N(\text{ion}) \Big/ \sqrt{\frac{\pi}{4\ln 2}}\,\Gamma\,. \tag{3}$$

We take the oscillator strength f (see Table 3) from Verner, Barthel, & Tytler (1994). This optical depth is to be compared with the rms noise level in the spectrum. For each line in each selected spectrum, the rms noise of the normalized spectrum [$\sigma(I)$] was calculated for a region about 20 Å wide (given in Table 3); these regions avoid strong absorption lines. The resulting rms value is inserted in the following formula to estimate the 1 σ error in the equivalent width, W, based on the error in fitting a Gaussian to an absorption line (Kaper et al. 1966):

$$\sigma(W) = \frac{\lambda}{c}\sqrt{3\sqrt{\frac{\pi}{8\ln 2}}}\,\sqrt{\Gamma h}\,\sigma(I)\,, \tag{4}$$

where Γ is the assumed line width of 15 km s^{-1} convolved with the instrumental resolution of 28 km s^{-1}, h is the grid spacing (5 km s^{-1}), and $\sigma(I)$ is the rms of the normalized spectrum. For a nondetection, we use this error estimate for the equivalent width as the 1 σ detection limit. It can be converted into a detection limit for the optical depth by solving the relation $W = \int \{1 - \exp[-\tau_0 f(v)]\} d\lambda$ for τ_0, assuming a Gaussian profile f(v) with a line width based on the intrinsic line width Γ corrected for the instrumental

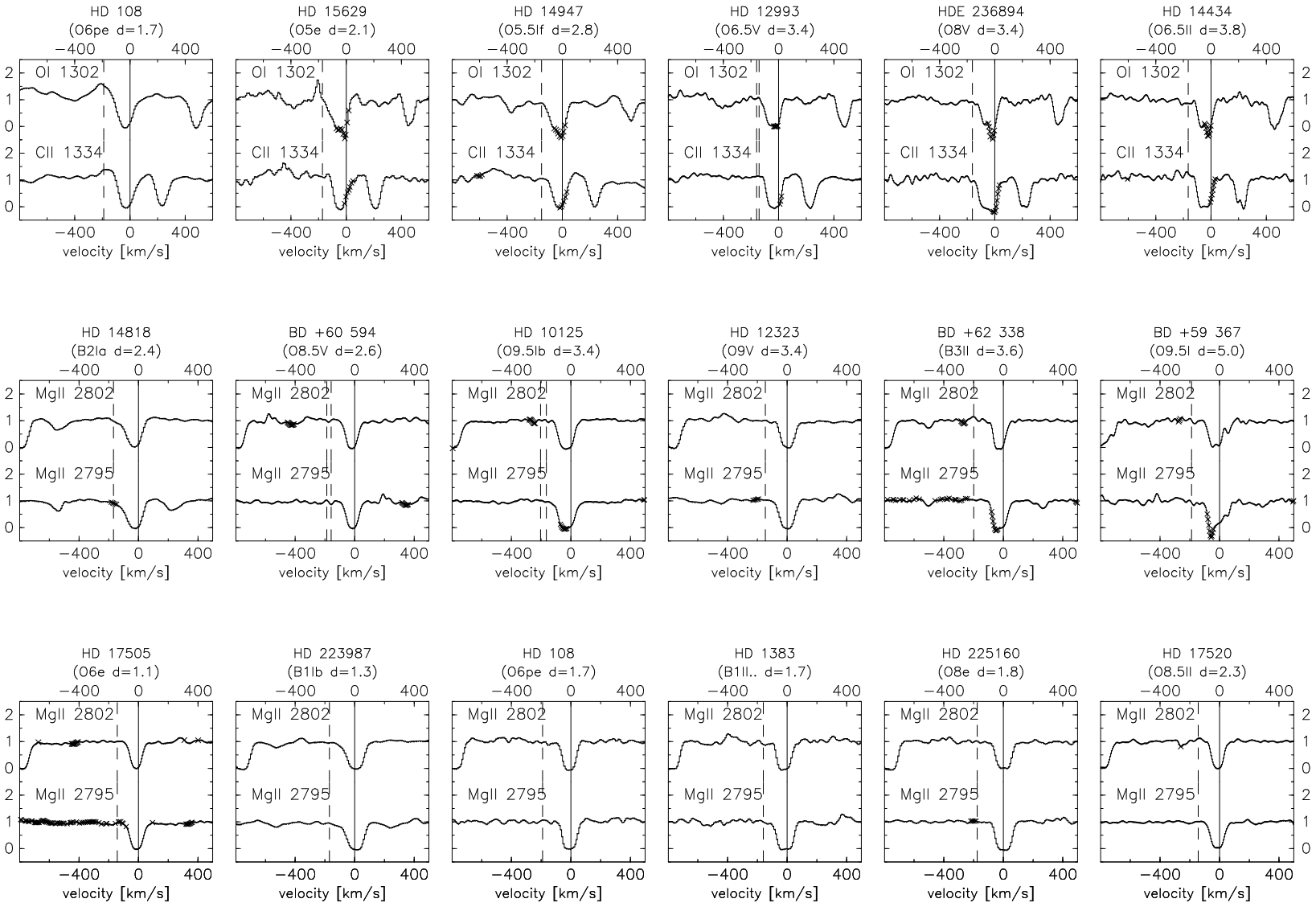

FIG. 4.—Zoom-in of a 1000 km s^{-1} wide region around each of the selected spectral lines, giving the normalized intensity as function of LSR velocity to show the absence of absorption due to HVC complex H. A velocity of 0 km s^{-1} is shown by the solid vertical lines, the LSR velocity of the HVC in the direction of the star by the dashed lines. The spectral type and distance of the star are given above each set of frames. The gas participating in differential galactic rotation shows clear absorption at velocities between about +20 and −100 km s^{-1}.

resolution. Thus, the rms noise can be converted into a 1 σ equivalent width error, which can be converted to a detection limit in the optical depth, giving the detection limit for the column density and the abundance. This can be compared to the predicted column density for the ion derived from the abundance, δ-value, and the H I column density. We give these detection limits at the 3 σ level.

3.2. *Detection Limits*

Table 4 gives the values for detection limits implied by the spectra. Columns (1)–(3) give the name of the star, the HVC velocity and the HVC column density as derived from the Effelsberg data, respectively. Column (4) gives the ion and line wavelength. Column (5) gives the S/N for that spectrum, calculated as the inverse of the rms, after normalization by the continuum (σ in eq. [4]). The predicted column density for the ion is given in column (6). The 3 σ detection limit in equivalent width (col. [7]) is found by inserting σ into equation (4) and multiplying by 3. The implied 3 σ detection limit for the column density (col. [8]) follows by solving the equivalent width for τ and inverting equation (3). Dividing by the H I column density gives the 3 σ detection limit in abundance (col. [9]). By dividing this by the solar abundance for the ion (from Table 3) we find the 3 σ detection limit for δ (col. [10]). The significance of the nondetection (S) is given as the ratio of the expected value of δ to the 1 σ detection limit for δ. The typical value of δ for low-velocity gas is used, as given in Table 3. Thus, S is the minimum factor by which the absorption is weaker than expected. If S is larger than 3, the nondetection is significant at the 3 σ level. If S is smaller than 3, the nondetection is not significant at the 3 σ level. All these quantities were calculated for many lines, but only for the lines included in Tables 3 and 4 is the nondetection usually significant. Figures 3*a* and 3*b* show 30 Å wide spectra around this final selection of lines, while Figure 4 shows a close-up of the relevant region for each of the lines. From these figures it is clear that no absorption associated with complex H can be discerned in any of the spectra. In the Mg II spectra of HD 14818, HD 223987, and BD +62 338, absorption is visible at 2791.50 and 2798.67 Å, which would correspond to a velocity of -520 km s^{-1} if they were Mg II $\lambda\lambda$2796, 2803 resonance lines. However, these lines instead originate from transitions between the first and second excited states of Mg^+ (see term diagram in Lang 1980, p. 139). They only occur for stars with spectral type between B0 and B8, being stronger in supergiants. If they occur, the λ2796 and λ2803 lines will be partly stellar. Other examples of these lines can be found, e.g., in de Boer et al. (1986).

4. DISCUSSION

4.1. *Distance Derivation*

Clearly, the nondetections are very significant for the Mg II, C II, and O I lines. For Mg II the significance ranges from a factor of 4100 (BD +62 338) to a factor of 53 (HD 14818); i.e., any absorption is at least 50 times weaker than expected. For the C II and O I lines, the significance of the nondetections ranges from 340 (HD 14947) to 32 (HD 14434). To estimate the significance of the nondetection for the Mg I lines a problem exists in that Mg^0 is usually not the dominant ionization stage. A very different value of δ is thus not hard to produce as the ratio Mg I/Mg II is unknown and may vary from cloud to cloud. Assuming that at most 10% of the Mg is neutral (the value assumed for Table 4), the Mg I nondetections are at least 4 times less significant than the Mg II nondetections. We conclude that the nondetections found from the spectra shown in Figures 3 and 4 are significant and, thus, that the HVC is probably behind each of the stars in Table 1. This conclusion cannot be made absolute, as we do not have spectra of extragalactic objects to confirm the presence of each of the analyzed ions. However, to explain all the nondetections as a result of lower intrinsic abundance would require that these abundances are a factor greater than 4100 (Mg) or greater than 340 (C) less than those found in low-velocity gas, which appears unlikely. Nondetections can also occur if the column density of the gas is depressed in the precise direction of a star. This also seems unlikely to be the case, as it would require a large depression of the H I column density, independently for each of 17 stars. Using our best distance estimates, the most distant star in our sample is BD +59 367, with a best distance estimate of 5.0 kpc. Garmany et al. (1982) gave a distance of 6.5 kpc. Even if its classification is slightly in error or if the extinction is different than our estimate, this star is at least 3.6 kpc distant. For five other stars, our best distance estimate is 3.4 kpc or more, with minimum distances of 3 kpc and maximum distances greater than 4.5 kpc. Thus, we feel confident in claiming that the distance to HVC complex H is larger than 3.4 kpc, and probably more than 5 kpc. If we were to use the distance to BD +59 367 given by Garmany et al. (1982), we might even conclude that the distance is above 6.5 kpc.

4.2. *Mass and Kinetic Energy*

The total gas mass of complex H can be estimated by summing over all detections in the Dwingeloo survey (Hulsbosch & Wakker 1988):

$$M = \sum 1.39 \cdot 0.236 \frac{T_B \Gamma}{R} d_{\rm kpc}^2 \, . \qquad (5)$$

Here we take into account a 28% helium fraction, giving the factor 1.39. The factor 0.236 converts a flux in Jy km s^{-1} to a mass in $M_\odot$. R is the conversion from brightness temperature to flux: $R = 0.158$ K Jy^{-1} for the Dwingeloo telescope (Hulsbosch & Wakker 1988). T_B is the brightness temperature of a detection, Γ an assumed line width (20 km s^{-1}); $d_{\rm kpc}$ is the distance in units of kpc. The resulting mass is $\sim 2.7 \times 10^4 d_{\rm kpc}^2$ $M_\odot$, or greater than 7×10^5 $M_\odot$, as $d > 5$ kpc. The total kinetic energy in complex H can also be estimated from the Dwingeloo survey data:

$$E_{\rm kin} = \sum_{\rm comp} \tfrac{1}{2} M_{\rm comp} (1.4 v_{\rm dev,\,comp})^2 \, , \qquad (6)$$

where the sum is over each of the profile components of the cloud separately. $M_{\rm comp}$ is the mass associated with each detection, converted from brightness temperature as in equation (5). The deviation velocity, $v_{\rm dev}$, was defined by Wakker (1991) and is the difference between the measured LSR velocity and the maximum velocity allowed by differential galactic rotation, i.e., the minimum peculiar velocity. A typical value of $v_{\rm dev}$ for a component of complex H is about 50 km s^{-1}, although deviations up to 90 km s^{-1} occur. The deviation velocity is the preferred velocity to use for this estimate of kinetic energy, rather than the velocity relative to the LSR or GSR, as it gives a minimum value. That is, if a cloud is at the edge of the Galaxy, the deviation

velocity gives the real peculiar velocity; if a cloud is more nearby, the peculiar velocity of the cloud relative to the surrounding ISM will be higher. The factor 1.4 in equation (6) tries to correct for a possible tangential velocity component, assumed to be equal to the radial component. Using this method, the total kinetic energy of complex H sums to about $2 \times 10^{44} d_{\rm kpc}^2$ J. Since complex H is not precisely circularly shaped, we estimate a typical diameter D from its total area, A: $D = (4A/\pi)^{1/2}$. Since the area is 480 square degrees (Wakker & van Woerden 1991), this implies $D = 25°$, or $430 d_{\rm kpc}$ pc. About a quarter of the mass and energy of complex H are contained in its core. If we only take the inner part of the complex, inside the 0.6 K contour, we find a core mass of $5 \times 10^3\ d_{\rm kpc}^2\ M_\odot$, kinetic energy of $5.5 \times 10^{43}\ d_{\rm kpc}^2$ J, and diameter of 6°.5, or $110\ d_{\rm kpc}$ pc.

4.3. *Interpretations*

As argued by Hulsbosch (1975) and by Wakker & van Woerden (1991), it seems likely that complex H is not strongly interacting with other galactic gas, as otherwise it is difficult to understand why there is so much cool neutral gas. An attempt to find Hα emission from ionized high-velocity gas is necessary to check this statement. Wakker & van Woerden (1991) argued that complex H is either a nearby structure inside the local bubble (Cox & Reynolds 1987) at a distance of at most a few 100 pc, or it is very distant, in the outskirts of the Galaxy (distance on the order of 10–30 kpc). Since the smaller distance is now excluded, we conclude that the HVC must be in or beyond the outskirts of the Galaxy. However, the data do not exclude that complex H is an H I cloud at a much larger distance, separate from the Galaxy; we discuss this possibility below, only to conclude that it is unlikely. One noteworthy property of complex H is the existence of a fairly regular velocity field, with the most negative velocities (-200 km s^{-1} relative to the LSR) near the center, decreasing to -120 km s^{-1} toward the outskirts (see Wakker & van Woerden 1991). Figure 5 shows crosscuts of the run of velocity with longitude and with latitude, taken through the center of the cloud. The shape of the velocity field is reminiscent of that of an expanding shell. There also seems to be a second embedded shell with a maximum velocity of -170 km s^{-1}. However, only one side is seen. Assuming that the expansion velocity is equal to the difference between the velocity in the center and that around the edges (80 km s^{-1}) the backside would have velocities of about -40 km s^{-1} and be hidden in the "normal" emission from the Galactic plane. On the other hand, a strong argument against an interpretation as a shell is that the brightest emission is seen near the center, rather than around the edges. This could indicate that the HVC consisted of a small dense cloud that hit the Galactic disk sideways, penetrated and accelerated previously present material. This situation is a variant of the ones discussed by Tenorio-Tagle et al. (1986). Without knowing the actual distance, explanations for the origin of HVC complex H are difficult to test. However, our distance limit and mass estimate do allow us to limit its possible origins. The main characteristics to be explained are (1) distance larger than 5 kpc, (2) large size ($\sim 25° \times 25°$); (3) location in the Galactic plane, (4) the velocities and brightness are largest near the center and show a rather regular drop toward the edges. With these characteristics in

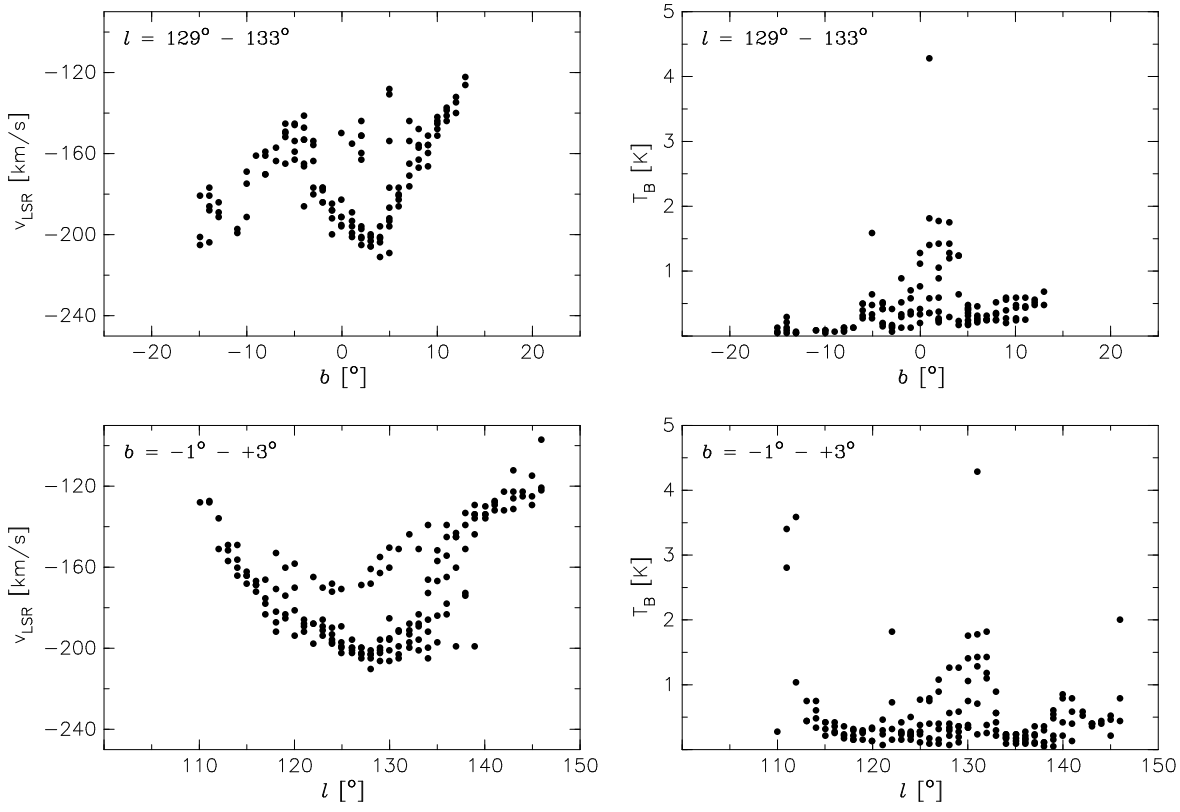

FIG. 5.—Crosscuts of the velocity field and the brightness distribution for 5° wide bands of constant latitude (*bottom*) or longitude (*top*)

mind, we discuss the following possible origins for HVC complex H.

a) *Complex H as the neutral edge of a superbubble.*—It is conceivable that regions of high-mass star formation exist in a spiral arm between the Perseus arm and the outer arm, and that a sequence of supernovae created a superbubble. Complex H could then represent the swept-up neutral gas around the edge of the superbubble. This hypothesis explains the shape of the velocity field, though not the distribution of column densities. It predicts that complex H is at a distance of about 6–9 kpc (Galactocentric radius 13–16 kpc). It should then be possible to find faint ($V = 11$–13) OB stars inside or behind the superbubble. Typical superbubbles have a diameter on the order of 100 pc, a swept-up mass of $1 \times 10^4\ M_\odot$ and mechanical energy of 1×10^{44} J (e.g., Oey 1996 and references therein). If complex H were a superbubble at 8 kpc distance, its diameter would be about 3.5 kpc and its mass about $2 \times 10^6\ M_\odot$, much larger than expected. Furthermore, a typical supernova will inject about 1% of 1×10^{44} J into the ISM. Since the total kinetic energy is $2 \times 10^{44}\ d_{\rm kpc}^2$ J, greater than $200\ d_{\rm kpc}^2$ supernovae are needed ($>10{,}000$ for $D = 8$ kpc) to accelerate all the observed mass in complex H to the observed peculiar velocities. This is an excessive number of supernovae. We therefore conclude that it is unlikely that HVC complex H represents a Galactic superbubble.

b) *Complex H is related to the outer arm.*—Around longitudes $l \sim 150$ there is a hint of a connection to the outer arm (see Wakker & van Woerden 1991). Thus, complex H could be at a Galactocentric radius comparable to that of the outer arm, which is 15 kpc (Haud 1992). This would put it 8.5 kpc from the Sun. At these Galactocentric radii, the HVC may behave similar to a cloud at large z-heights. It would be a fast-moving cloud moving through a tenuous surrounding neutral medium into an ever denser medium, as it penetrates toward smaller Galactocentric radii. This might explain why the fine structure is similar to that seen in high-latitude HVCs (Wakker & Schwarz 1991). However, it does not fit in Haud's (1992) model for the outer arm. Thus, since a model in which complex H is somehow related to the outer arm provides no natural explanation for the peculiar velocities, velocity field, and column density distribution of complex H, on balance it does not seem likely.

c) *Complex H is a Galactic fountain HVC.*—The average deviation velocity of an H-atom in the cloud is about 50 km s^{-1}. This is a typical velocity for a neutral hydrogen atom in 1×10^5 K gas. In the Galactic fountain model, the Galaxy is assumed to be surrounded by a hot ($>5 \times 10^5$ K) gaseous halo, in which instabilities occur and condensations are formed (e.g., Houck & Bregman 1990). This thermal energy can be converted to bulk motions and when neutral clouds form, their velocity can range up to about 80 km s^{-1}. They are subsequently accelerated by the Galactic gravitation field. If a condensation were to form at a large Galactocentric radius, it is likely that its velocity would develop a large component directed toward the Galactic center. Objects like HVC complexes A and C are often assumed to have formed in a fountain, and their masses are on the order of 10^5–$10^6\ M_\odot$ (Wakker & van Woerden 1997), similar to that of complex H if it is at a distance of less than 8 kpc (Galactocentric radius less than 15 kpc). Thus, the energy and mass content of complex H are consistent with the hypothesis that it formed within a Galactic fountain, with the only special property being that it formed in the outskirts of the Galaxy. Its current position near the Galactic plane does not necessarily imply that it formed near it, as it may have a large tangential velocity perpendicular to the Galactic plane and may just happen to cross it at the current time. Nevertheless, it is more likely that the radial velocity with respect to the Galactic center and the Sun is now larger than the velocity perpendicular to the plane. It is further possible that the original condensation was quite dense and corresponds to what is now the core of complex H. The outskirts of complex H then would consist of accelerated disk gas. The systematic appearance of the velocity field would be a consequence of the disk gas being pushed away. Such a situation is similar to the ones covered by Tenorio-Tagle et al. (1986), who described the consequences to the disk of a cloud bullet hitting it from above. To further test this hypothesis requires (1) models similar to those of Tenorio-Tagle et al. (1986), but for the situation of a hydrogen bullet hitting the Galactic plane from the side, and (2) better models for the Galactic fountain in order to check whether it is possible to create a condensation that would have the velocity implied for complex H.

d) *Complex H is an infalling extragalactic cloud.*—This hypothesis assumes that there are small ($M < 10^7\ M_\odot$) H I clouds in the Local Group, possibly satellites of the Milky Way, of which complex H used to be one. It now is close to the Milky Way and in the process of passing by or being accreted. Concerning the morphology and most other characteristics, this hypothesis is indistinguishable from (*c*). The difference lies in the origin of the gas. In (*c*) the original cloud consists of cooled-down Galactic halo gas, while now the original cloud was extragalactic. A suggestion that HVCs are extragalactic was presented recently by Blitz et al. (1997). They claimed that "the HVCs are remnants of Local Group formation" and "most plausibly explained as members of the Local Group of galaxies." Although no details of this work have been published, their arguments appear to be of a statistical nature and carry no weight for individual HVCs. What is required is a direct distance determination for individual HVCs. For the case of complex H we show below (models *e* and *f*) that it would be unrealistically massive if it were a Local Group object at a distance of more than 50 kpc. A measurement of the *intrinsic* metallicity of the HVC may also be helpful: a high metallicity would argue against the Blitz et al. (1997) model, a low metallicity (<0.1 solar) would be compatible with it. This requires a detection of sulphur or zinc absorption in the UV spectrum of an extragalactic probe (see Wakker & van Woerden 1997). Unfortunately, since the brightest such probe of complex H has $B = 16$, this is currently an impossible observation, as *HST*/STIS can observe only objects brighter than about $B = 14.5$.

e) *Complex H as the* H I *component of a dwarf galaxy.*—We next consider the possibility that complex H might be the H I component of a dwarf companion of the Milky Way. In its direction Galactic extinction is about 0.6 mag kpc^{-1} (Lucke 1978). Assuming that the extinction decreases exponentially with radius with a scale length of 3.8 kpc (Mathis, Mezger, & Panagia 1983), the optical image of complex H would suffer about 2.5 mag of extinction, and the possible dwarf galaxy would be very difficult to detect because of the large number of Galactic foreground stars. For various assumed distances of complex H, we shall compare its properties with those of dwarf irregular galaxies in the Local Group; because of their lack of H I, dwarf ellipticals

and dwarf spheroidals are clearly disqualified. Hodge (1994) gives a listing of Local Group members; for the irregular galaxies we take H I masses ($M_{\rm H\,I}$), rotation speeds ($W_R/2$), total masses (M_T), and H I mass fractions ($M_{\rm H\,I}/M_T$) from Tully (1988). Another useful comparison is to irregular galaxies outside the Local Group, as measured at Westerbork by Broeils & van Woerden (1994, hereafter BvW). For assumed distances of 5, 10, 30, and 100 kpc, the H I mass of complex H would be 0.05, 0.2, 1.7, and $19 \times 10^7\ M_\odot$, respectively. The Local Group irregulars have H I masses ranging from 0.4 to $90 \times 10^7\ M_\odot$, with five out of 11 values between 5×10^7 and 8×10^7; the BvW field irregulars have H I masses between 6×10^7 and $300 \times 10^7\ M_\odot$. Thus, the H I mass of complex H would be comparable to the majority of the Local Group dwarfs for a distance of order 60 kpc, similar to that of the (more massive) Magellanic Clouds. The observed dispersion $[\langle (v_{\rm LSR} - \bar{v}_{\rm LSR})^2 \rangle^{1/2}]$ of radial velocities in complex H is 27 km s^{-1}, corresponding to a 20% width W_R of 100 km s^{-1}. The Local Group dwarfs have W_R values between 30 and 120 km s^{-1}, the BvW irregulars between 50 and 130 km s^{-1}. Thus, averaged over the whole complex, the internal motions in complex H are at the high end of those for dwarf irregular galaxies; they are comparable to galaxies of blue absolute magnitude around -16 (Rhee 1996). The angular diameter of complex H seen in Figure 1 is of order 25°, equivalent to values between 2 and 40 kpc for distances between 5 and 100 kpc. However, these values are not directly comparable to the H I diameters of galaxies, which are usually standardized at a surface density of 1 $M_\odot$ pc^{-2}, or $N_{\rm H\,I} = 1.25 \times 10^{20}$ cm^{-2}; complex H reaches such surface densities only at its brightest spots. Thus, while the BvW irregulars have H I diameters of 5–40 kpc, the corresponding H I diameter of complex H would be at most of order 0.5–10 kpc, for distances between 5 and 100 kpc. Complex H does not show a velocity gradient indicative of rotation, unlike the irregular galaxies. We therefore need to apply the virial theorem to estimate the total mass of complex H: $M_T \sim 6\ \sigma_V^2\ R/G$, with velocity dispersion $\sigma_V = 27$ km s^{-1}, and radius $R = 12°$, or $0.2\ d_{\rm kpc}$. For distances between 5 and 100 kpc, this yields total masses between 1.1 and $22 \times 10^9\ M_\odot$. Local Group dwarfs have M_T values in the range $(0.04\text{–}3) \times 10^9\ M_\odot$, and BvW irregulars have $(0.13\text{–}22) \times 10^9\ M_\odot$. Hence the M_T value derived for complex H exceeds that of almost all Local Group dwarfs for any distance greater than 5 kpc and is comparable to that of the more massive field irregulars. This is clearly a result of the large velocity spread observed in complex H; and the assumption of virial equilibrium is probably not justified, especially if the kinematics of the hypothesized dwarf galaxy is disturbed by its proximity to the Milky Way. Depending on distance, the $M_{\rm H\,I}/M_T$ ratio would lie between 0.4 and 9×10^{-3}, which is far below the ranges for Local Group dwarfs (0.05–0.5) and for BvW irregulars (0.1–1). The significance of this discrepancy depends, of course, again on the assumptions made in deriving M_T. In summary, the observed and derived properties of complex H do not support an interpretation as a dwarf irregular satellite of the Milky Way, unless its structure and kinematics are strongly disturbed by the latter. In this connection, it is relevant to compare complex H to the Sagittarius (Sgr) dwarf galaxy recently discovered by Ibata, Gilmore, & Irwin (1994) on sky survey plates. This dwarf, located 16 kpc from the Galactic center and 24 kpc from the Sun, has an absolute magnitude of about -13 and a stellar population consisting of old and intermediate ages; no H I has been found associated with it. The Sgr dwarf is strongly elongated, with axial ratio about 1:3; its shape and short distance, together with orbit calculations, suggest that it is being tidally disrupted (Johnston, Spergel, & Hernquist 1995; Velazquez & White 1995). However, there is no strong similarity between complex H and the Sagittarius dwarf. Complex H is not strongly elongated. It lacks the linear velocity gradient predicted in models by Johnston et al. (1995). It also lacks the (accidental) constant radial velocity observed in the Sgr dwarf, as well as its small velocity dispersion of 10 km s^{-1}. Rather, the velocity field of complex H bears the strong signature of an expanding shell.

f) *Complex H as an intergalactic cloud in the Local Group.*—Both the position on the sky and the radial velocity of complex H are fairly close to those of the galaxies M31 (angular separation of 24°, $v_{\rm LSR} = -294$ km s^{-1}, distance 715 kpc), M33 (33°, -183 km s^{-1}, 790 kpc), and IC 10 (12°, -337 km s^{-1}, 1.25 Mpc). If we would put complex H at a similar distance of 1 Mpc, its H I mass would be $2 \times 10^{10}\ M_\odot$, exceed that of every galaxy in the Local Group, and be similar to the *total* mass of M33. Assuming again virial equilibrium—which seems better justified in this case—the total mass of complex H would be $2 \times 10^{11}\ M_\odot$, far exceeding that of M33, and approaching that of the giant spirals, M31 and Milky Way. The ratio $M_{\rm H\,I}/M_T$ would be about 0.10 and be similar to that of the large, late-type galaxies M33 and IC 10. The size of complex H would be as much as 400 kpc. No intergalactic clouds of such large size, H I mass, and total mass have been found in nearby galaxy groups.

5. CONCLUSIONS

We analyzed all *IUE* spectra of objects projected onto HVC complex H. This is one of the largest HVCs, but unlike other HVCs it is in the Galactic plane, centered on a longitude of 131°. For 17 stars, a clean Mg II, C II, or O I spectrum with signal-to-noise ratio greater than 5 can be found. None of these spectra shows absorption at the velocity of the HVC. We derive abundance limits for the HVC and compare these to the gaseous abundances in low-velocity gas, and find that the observed detection limits are 30–4100 times lower. This strongly suggests that the nondetections are the result of the stars being in front of the HVC. To be absolutely certain we would need to detect Mg II, C II, or O I absorption in the spectrum of an extragalactic object projected onto complex H, but such data do not exist, because of a lack of sufficiently bright extragalactic probes. This is unfortunate, since in practice the only way to definitively decide between a Galactic and an extragalactic origin for a HVC may be through a determination of intrinsic elemental abundances. The lower limit to the distance of HVC complex H implied by the nondetections is at least 3.4 kpc, probably 5 kpc and possibly 6.5 kpc. This suggests that the cloud is in the outer parts of the Galactic disk or beyond. Using the lower limits on the mass, kinetic energy, and radius that we can set, we considered several explanations: (*a*) the HVC is the neutral edge of a superbubble at a large Galactocentric radius; (*b*) it is related to the outer arm; (*c*) it is an infalling "normal" HVC associated with the Galactic fountain, but one that formed at a very large Galactocentric radius and whose orbit happened to take it to the Galactic plane; (*d*) it is an infalling intergalactic cloud; (*e*) it is the H I component of a nearby dwarf galaxy;

or (*f*) it is an intergalactic cloud in the Local Group. We conclude that (*a*), (*b*), (*e*), and (*f*) are unlikely but that (*c*) and (*d*) are possible.

H. v. W. wishes to thank Domitilla de Martino and the staff of the ESA Satellite Tracking Station, Villafranca, Spain, for their excellent support during his observing run in 1993 November. He is also grateful to Renée Kraan-Korteweg, René Oudmaijer, and Ulrich Schwarz for their help with the preparation of the observations. The Effelsberg Telescope belongs to the Max Planck Institut für Radio Astronomie at Bonn. This research has made use of the Simbad database, operated at CDS, Strasbourg, France.

REFERENCES

Anders, N., & Grevesse, E. 1989, Geochim. Cosmochim. Acta, 53, 1973
Apparao, K. M. V., et al. 1978, Nature, 273, 450
Blitz, L., Spergel, D. N., Teuben, P. J., Hartmann, L., & Burton, W. B. 1997, BAAS, 28, 1349
Broeils, A. H., & van Woerden, H. 1994, A&AS, 107, 129
Buscombe, W. 1995, MK Spectral Classifications, General Catalogue (4th version; Evanston: Northwestern Univ.)
Cardelli, J. A., Meyer, D. M., Jura, M., & Savage, B. D. 1996, ApJ, 467, 334
Centurión, M., Vladilo, G., de Boer, K. S., Herbstmeier, U., & Schwarz, U. J. 1994, A&A, 292, 261
Cox, D. P., & Reynolds, R. J. 1987, ARA&A, 25, 303
de Boer, K. S., Lenhart, H., van der Hucht, K. A., Kamperman, T. M., Kondo, Y., & Bruhweiler, F. C. 1986, A&A, 157, 119
Fitzgerald, M. P. 1970, A&A, 4, 234
Fitzpatrick, E. L. 1997, ApJ, 482, L199
Garmany, C. D., Conti, P. S., & Chiosi, C. 1982, ApJ, 263, 777
Hardorp, J., Rohlfs, K., Slettebak, A., & Stock, J. 1959, Luminous Stars in the Northern Milky Way. I. (Hamburg-Bergedorf: Hamburger Sternwarte and Warner and Swasey Obs.)
Haud, U. 1992, MNRAS, 257, 70
Hodge, P. W. 1994, in The Formation and Evolution of Galaxies, ed. C. Muñoz-Tunon & F. Sanchez (Cambridge: Cambridge Univ. Press), 1
Houck, J. C., & Bregman, J. N. 1990, ApJ, 352, 506
Hulsbosch, A. N. M. 1971, A&A, 14, 489
———. 1975, A&A, 40, 1
Hulsbosch, A. N. M., & Wakker, B. P. 1988, A&AS, 75, 191
Ibata, R. A., Gilmore, G., & Irwin, M. J. 1994, Nature, 370, 194
Jenkins, E. B. 1987, in Interstellar Processes: Proceedings of the Symposium on Interstellar Processes, Grand Teton National Park, 1986 July (Dordrecht: Reidel), 533
Johnston, K. V., Spergel, D. N., & Hernquist, L. 1995, ApJ, 451, 598
Kalberla, P. M. W., Mebold, U., & Reich, W. 1980, A&A, 82, 275
Kalberla, P. M. W., Mebold, U., & Reif, K. 1982, A&A, 106, 190
Kaper, H. G., Smits D. W., Schwarz, U. J., Takakubo, K., & van Woerden, H. 1966, Bull. Astr. Inst. Netherlands, 18, 465
Keenan, F. P., Shaw, C. R., Bates, B., Dufton, P. L., & Kemp, S. N. 1995, MNRAS, 272, 599
Lang, K. R. 1980, Astrophysical Formulae: A Compendium for the Physicist and Astrophysicist (2d corr. and enlarged ed.; Berlin: Springer)
Lucke, P. B. 1978, A&A, 64, 367
Mathis, J. S., Mezger, P. G., & Panagia, N. 1983, A&A, 128, 212
Meyer, D. M., Jura, M., Hawkins, I., & Cardelli, J. A. 1994, ApJ, 437, L59
Muller, C. A., Oort, J. H., & Raimond, E. 1963, Comptes Rendues Acad. Sci. Paris, 257, 1661
Oey, M. S. 1996, ApJ, 467, 666
Rhee, M. H. 1996, Ph.D. thesis, Rijks Universiteit, Groningen
Robertson, J. G., Schwarz, U. J., van Woerden, H., Murray, J. D., Morton, D. C., & Hulsbosch, A. N. M. 1991, MNRAS, 248, 508
SAO Staff. 1966, Smithsonian Astrophysical Observatory (SAO) Star Catalog (Cambridge: SAO)
Savage, B. D., & Sembach, K. R. 1996, ARA&A, 34, 279
Schwarz, U. J., Wakker, B. P., & van Woerden, H. 1995, A&A, 302, 364
Straizys, V., & Kurilene, G. 1981, Ap&SS, 80, 353
Tenorio-Tagle, G., Bodenheimer, P., Różyczka, M., & Franco, J. 1986, A&A, 170, 107
Tully, R. B. 1988, Nearby Galaxy Catalog (Cambridge: Cambridge Univ. Press)
Turon, C., Gómes, A., Crifo, F., Créze, M., Perryman, M. A. C., Morin, D., Arenou, F., Nicolet, B., Charetou, M., & Egret, D. 1992, A&A, 258, 88
Velazquez, H., & White, S. D. M. 1995, MNRAS, 275, L23
Verner, D. A., Barthel, P. D., & Tytler, D. 1994, A&AS, 108, 287
Véron-Cetty, M.-P., & Véron, P. 1993, Quasars and Active Galactic Nuclei, 6th ed., ESO Sci. Rep. 13
Wakker, B. P. 1991, A&A, 250, 499
Wakker, B. P., & Schwarz, U. J. 1991, A&A, 250, 484
Wakker, B. P., & van Woerden, H. 1991, A&A, 250, 509
———. 1997, Ann. Rev. A&A, 35, 217
Wakker, B. P., van Woerden, H., Schwarz, U. J., Peletier, R. F., & Douglas, N. G. 1996, A&A, 306, L25
Wakker, B. P., Vijfschaft, B., & Schwarz, U. J. 1991, A&A, 249, 233
Walborn, N. R. 1973, AJ, 78, 1067
West, K. A., Pettini, M., Penston, M. V., Blades, J. C., & Morton, D. C. 1985, MNRAS, 215, 481